

Three-dimensional Guidance Law for Formation Flight of UAV

Byoung-Mun Min* and Min-Jea Tahk**

* Department of Aerospace Engineering, KAIST, Daejeon, Korea
(Tel : +82-42-869-3789; E-mail: bmmmin@fdcl.kaist.ac.kr)

**Department of Aerospace Engineering, KAIST, Daejeon, Korea
(Tel : +82-42-869-3718; E-mail: mjtahk@fdcl.kaist.ac.kr)

Abstract: In this paper, the guidance law applicable to formation flight of UAV in three-dimensional space is proposed. The concept of miss distance, which is commonly used in the missile guidance laws, and Lyapunov stability theorem are effectively combined to obtain the guidance commands of the wingmen. The propose guidance law is easily integrated into the existing flight control system because the guidance commands are given in terms of velocity, flight path angle and heading angle to form the prescribed formation. In this guidance law, communication is required between the leader and the wingmen to achieve autonomous formation. The wingmen are only required the current position and velocity information of the leader vehicle. The performance of the proposed guidance law is evaluated using the complete nonlinear 6-DOF aircraft system. This system is integrated with nonlinear aerodynamic and engine characteristics, actuator servo limitations for control surfaces, various stability and control augmentation system, and autopilots. From the nonlinear simulation results, the new guidance law for formation flight shows that the vehicles involved in formation flight are perfectly formed the prescribed formation satisfying the several constraints such as final velocity, flight path angle, and heading angle.

Keywords: guidance law, formation flight, UAV, Lyapunov stability theorem, nonlinear aircraft system, nonlinear simulation

1. INTRODUCTION

The problem of autonomous formation flight of unmanned aerial vehicle(UAV) has been widely studied in the past several years. Giulietti et al.[1], addressed dynamic modeling and formation flight control considering aerodynamic effects due to the vortices. A Similar approach had done Pacher and coworkers [2]. In their work, a tight formation control system for wingman was designed based on aerodynamic coupling effects caused by leader’s vortex. An adaptive approach to vision based UAV formation control using estimated line of sight(LOS) range was proposed by Sattigeri and Calies [3]. Tahk, Park, and Ryoo [4] suggested LOS guidance law for formation flight. The synthesized standard LQ-based structure for formation position error control in close-formation flight of autonomous aircraft was described in Ref. [5]. The formation-keeping control problem for the three-dimensional autonomous formation flight was addressed in Ref. [6]. There are many other previous work about the problem of autonomous formation flight. However, the most previous results are restricted to two-dimensional formation problem and full nonlinear dynamics of the considered aircraft model is not reflected, perfectly. Also, it cannot guarantee the performance of maintenance formation form while the leader maneuvering with lateral acceleration.

Therefore, the motivation of this paper is to propose a guidance law for three-dimensional formation. The proposed guidance law generates velocity and flight path angle commands in longitudinal direction, and heading angle command in lateral direction to form the prescribed formation form. Thus, the proposed guidance law can be easily applied to the existing aircraft flight control system.

This paper is organized as follows. In the next section, 6-DOF aircraft’s dynamic and the nonlinear aircraft system used in formation flight simulation are briefly mentioned. In section 3, the guidance law for formation flight is derived based on the concept of miss distance and Lyapunov stability theorem. The constructed nonlinear simulation model for formation flight is introduced in this section. Simulation scenario and simulation result applying the proposed guidance law to formation flight are presented in section 4, followed by conclusion in section 5.

2. NONLINEAR 6-DOF AIRCRAFT SYSTEM

2.1 Equation of motion

Generally, the equation of translational and rotational motion of an aircraft can be derived from Newton’s second law of motion [7].

$$F = m \frac{dV}{dt} \Big|_E = m \left[\frac{dV}{dt} \Big|_B + \omega_{BE} \times V \right] \tag{1}$$

$$H = \frac{dH}{dt} \Big|_E = \left[\frac{dH}{dt} \Big|_B + \omega_{BE} \times H \right] \tag{2}$$

where $\Big|_E$ and $\Big|_B$ represent time derivative with respect to earth-frame and body-frame, respectively. F and M are the force and moment generated by gravity, thrust, and aerodynamics. Considering aircraft model in this paper has fully nonlinear aerodynamic and engine characteristic coefficients in the form of two or three dimensional look-up table. The detailed information about these coefficients is referred in Ref. [8].

2.2 Nonlinear aircraft system

Fig. 1 represents the nonlinear aircraft system, which is integrated various stability and control augmentation system (SCAS) and autopilots based on 6-DOF aircraft dynamics.

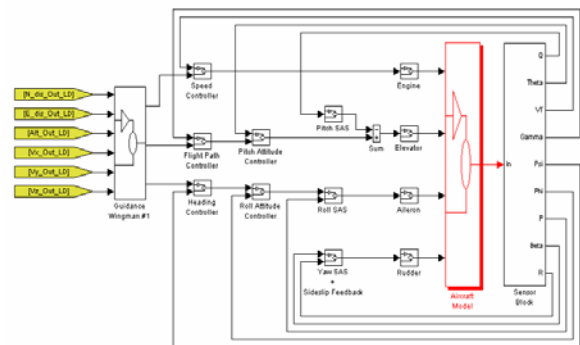


Fig. 1 Simulation model of nonlinear aircraft system

All components of these SCAS and autopilots were designed using classical control method as explained in Stevens [7]. Each actuator servo and throttle are modeled as a first-order lag system and their operation ranges are limited within its upper and lower saturation positions. However, the nonlinear nature of aerodynamic and engine characteristics are sufficiently captured by using two or three dimensional linear interpolation during nonlinear simulation. The full information about controller type and its gain are mentioned in Ref. [8].

3. DERIVATION OF GUIDANCE LAW

3.1 Guidance law for formation flight

The proposed guidance law for formation flight is based on the miss distance concept [9] widely used in missile guidance law and Lyapunov stability theorem [10]. This concept has been successfully implemented in deriving the guidance law for Bank-To-Turn missile [11] and in control problem of autonomous vehicles in longitudinal platoons [12].

Referring to Fig. 2, we assume that wingman is chasing leader in three dimensional space. In this situation, the desired position of wingman to form the formation flight is defined from leader with fixed relative distance. We define the expected miss distance vector between wingman and the desired position for formation flight at t_{go} as

$$d_{t_{go}} = (d^L - d^F - d^W) + (v^L - v^W)t_{go} \quad (3)$$

where superscript L and W denote 'leader' and 'wingman', respectively, and t_{go} is the time-to-go until the fixed future time t_f . Eq. (3) can be rewritten as

$$d_{t_{go}} = M_x e_x + M_y e_y + M_z e_z \quad (4)$$

where (e_x, e_y, e_z) are the unit direction vectors of the fixed reference frame. Each vector component M_x, M_y, M_z denotes as

$$M_i = (d_i^L - d_i^F - d_i^W) + (v_i^L - v_i^W)t_{go}, \quad i = x, y, z \quad (5)$$

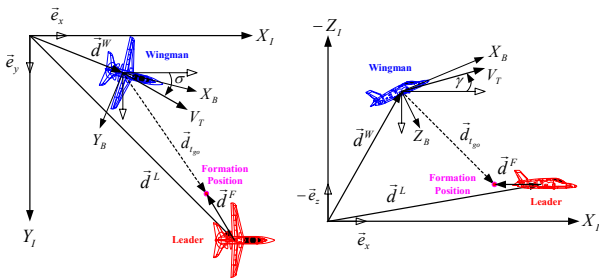


Fig. 2 The chasing geometry of leader and wingman

To derive guidance law for formation flight using Lyapunov stability theorem, we introduce a positive definite Lyapunov function candidate, which is composed of expected miss distance vector, as follows.

$$V = \frac{1}{2} d_{t_{go}} \cdot d_{t_{go}} \quad (6)$$

Differentiation of Eq. (6) yields

$$\frac{dV}{dt} = M_x (\dot{v}_x^L - \dot{v}_x^W)t_{go} + M_y (\dot{v}_y^L - \dot{v}_y^W)t_{go} + M_z (\dot{v}_z^L - \dot{v}_z^W)t_{go} \quad (7)$$

In the fixed reference frame, the velocity vector of wingman v^W , under the assumption of perfect coordinate

turn maneuver: $\sigma = \psi + \beta \approx \psi$, can be written as

$$\begin{aligned} v^W &= v_x^W e_x + v_y^W e_y + v_z^W e_z \\ &= v \cos \gamma \cos \sigma e_x + v \cos \gamma \sin \sigma e_y - v \sin \gamma e_z \\ &\approx v \cos \gamma \cos \psi e_x + v \cos \gamma \sin \psi e_y - v \sin \gamma e_z \end{aligned} \quad (8)$$

where v is the total speed of wingman, γ and ψ denote flight path and heading angles of wingman, respectively.

Differentiates Eq. (8) and substitutes it into Eq. (7) yields

$$\begin{aligned} \frac{dV}{dt} &= (M_x \dot{v}_x^L + M_y \dot{v}_y^L + M_z \dot{v}_z^L +)t_{go} \\ &\quad - \dot{v} (M_x \cos \psi \cos \gamma + M_y \sin \psi \cos \gamma - M_z \sin \gamma)t_{go} \\ &\quad - v \dot{\psi} \cos \gamma (-M_x \sin \psi + M_y \cos \psi)t_{go} \\ &\quad - v \dot{\gamma} (M_x \cos \psi \sin \gamma + M_y \sin \psi \sin \gamma + M_z \cos \gamma)t_{go} \end{aligned} \quad (9)$$

Now, we introduce a control frame with the unit direction vector (e_v, e_ψ, e_γ) as depicted in Fig. 3. In control frame, the direction of e_v is along the current velocity vector, the direction of e_ψ is perpendicular to e_v and positive in the sense of increasing heading angle, and e_γ is completely determined by the right-hand rule and its positive direction is along the decreasing flight path angle. Then, the direction cosine matrix between the fixed reference frame and control frame can be defined as follows

$$\begin{bmatrix} e_v \\ e_\psi \\ e_\gamma \end{bmatrix} = \begin{bmatrix} \cos \gamma \cos \psi & \cos \gamma \sin \psi & -\sin \gamma \\ -\sin \psi & \cos \psi & 0 \\ \sin \gamma \cos \psi & \sin \gamma \sin \psi & \cos \gamma \end{bmatrix} \begin{bmatrix} e_x \\ e_y \\ e_z \end{bmatrix} \quad (10)$$

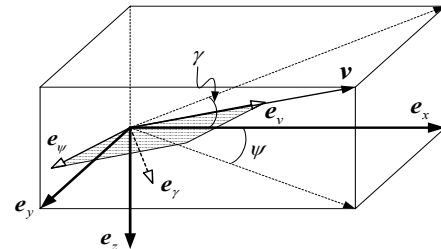


Fig. 3 Orientation of fixed reference frame and control frame

Using this the direction cosine matrix, Eq. (9) will be simplified as

$$\frac{dV}{dt} = M_v (\dot{v}_v^L - \dot{v})t_{go} + M_\psi (\dot{v}_\psi^L - v \dot{\psi} \cos \gamma)t_{go} + M_\gamma (\dot{v}_\gamma^L + v \dot{\gamma})t_{go} \quad (11)$$

In Eq. (11), the dynamic characteristics of the three control loops for speed v , flight path angle γ , and heading angle ψ should be explicitly identified. However, using the full explicit these dynamic equations is impossible due to its complexity and highly coupled longitudinal-lateral dynamics. To avoid these difficulties, we assume that each control loop can be represented as first-order lag system as

$$\begin{aligned} \dot{v} &= \frac{1}{\tau_v} (v_c - v) \\ \dot{\gamma} &= \frac{1}{\tau_\gamma} (\gamma_c - \gamma) \\ \dot{\psi} &= \frac{1}{\tau_\psi} (\psi_c - \psi) \end{aligned} \quad (12)$$

where τ_v , τ_γ , and τ_ψ denote the time constants of each control loop, which is determined by least square regression method using fully nonlinear simulation data about step input.

Substituting Eq. (12) into Eq. (11) yields

$$\begin{aligned} \frac{dV}{dt} = & M_v \left[\dot{v}_v^L - \frac{1}{\tau_v} (v_c - v) \right] t_{go} + \\ & M_\psi \left[\dot{\psi}_\psi^L - v \cos \gamma \frac{1}{\tau_\psi} (\psi_c - \psi) \right] t_{go} + \\ & M_\gamma \left[\dot{\gamma}_\gamma^L + v \frac{1}{\tau_\gamma} (\gamma_c - \gamma) \right] t_{go} \end{aligned} \quad (13)$$

To satisfy the Lyapunov stability theorem, Eq. (6) is positive definite and Eq. (13) is negative definite, simultaneously. So, we can appropriately select the guidance command for each control loop that Eq. (13) has negative definiteness. One of the choice of these guidance commands is possibly to get as follows

$$\begin{aligned} \frac{dV}{dt} = & M_v \left[\dot{v}_v^L - \frac{1}{\tau_v} (v_c - v) \right] t_{go} + \\ & M_\psi \left[\dot{\psi}_\psi^L - v \cos \gamma \frac{1}{\tau_\psi} (\psi_c - \psi) \right] t_{go} + \\ & M_\gamma \left[\dot{\gamma}_\gamma^L + v \frac{1}{\tau_\gamma} (\gamma_c - \gamma) \right] t_{go} \\ = & -N (M_v^2 + M_\psi^2 + M_\gamma^2) \end{aligned} \quad (14)$$

where N is an arbitrary positive value.

Consequently, the guidance commands for each control loop are determined as follows

$$v_c = v + \frac{N}{t_{go}} \tau_v M_v + \tau_v \dot{v}_v^L \quad (15)$$

$$\psi_c = \psi + \frac{N}{t_{go}} \frac{\tau_\psi}{v \cos \gamma} M_\psi + \frac{\tau_\psi}{v \cos \gamma} \dot{\psi}_\psi^L \quad (16)$$

$$\gamma_c = \gamma - \frac{N}{t_{go}} \frac{\tau_\gamma}{v} M_\gamma - \frac{\tau_\gamma}{v} \dot{\gamma}_\gamma^L \quad (17)$$

3.2 Construction simulation model for formation flight

Nonlinear simulation model for formation flight is shown in Fig. 4. In this paper, one leader and two wingmen models are considered applying the proposed guidance law to formation flight simulation. In this simulation model, we assume that each wingman receives broadcasting position and velocity data from the leader aircraft in real time without any communication delay. In Fig. 4, all aircraft system i.e. *Leader*, *Wingman 1*, and *Wingman 2*, have the same dynamic characteristics and control structure illustrated in Fig. 1 at section 2.

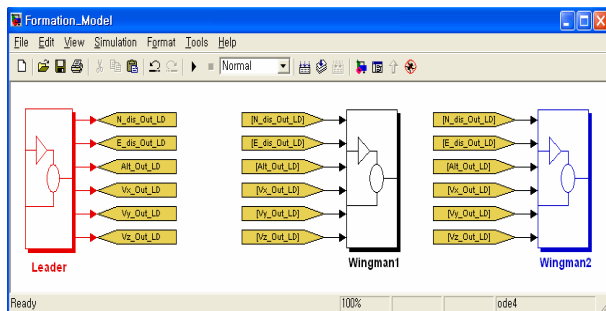


Fig. 4 Nonlinear simulation model for formation flight

4. SIMULATION RESULT AND ANALYSIS

4.1 Determination of optimal spacing in formation flight

Generally, the formation geometry is determined by the leader's position relative to the wingman in three dimensional space. Thus the vortex created by leader exerts aerodynamic forces and moments on wingman in formation flight. It is well known that wingman can reduce the fuel consumption and increase the mission range by maintaining proper formation position. By these reason, determining the optimal position of wingman is very important in formation flight. In this paper, the optimal spacing of wingman in formation flight can be determined by horseshoe vortex model in Ref.[2]. From Ref. [2], the optimal spacing of wingman is calculated as $\bar{x}=2b$, $\bar{y}=(\pi/4)b$, and $\bar{z}=0$, where b is the wingspan of the leader aircraft. The wingspan of leader aircraft considering in this paper is 119 ft , the optimal spacing is specified by $\bar{x}=238\text{ ft}$, $\bar{y}=\pm 93.5\text{ ft}$, and $\bar{z}=0\text{ ft}$, respectively.

4.2 Simulation scenario

Simulation scenario to evaluate the performance of the proposed guidance law is summarized in Fig. 5. In this simulation scenario, initially, three aircrafts fly from arbitrary position, and the end of *Formation 1*, three aircrafts are formed triangular formation form maintaining the optimal spacing at 1500ft altitude with 270 ft/sec velocity. At the end of *Formation 1*, the leader aircraft decreases velocity and altitude at 250 ft/sec and 800 ft , respectively. During this *Formation 2* stage, the formation form is changing to diagonal form. In the final formation phase *Formation 3*, the leader aircraft performed lateral acceleration maneuver. In this time, two wingmen change its position each other maintaining the diagonal formation form at different altitude. The final formation position in *Formation 3* phase is not the optimal spacing because the relative distance of each wingman is non-zero in z-direction.

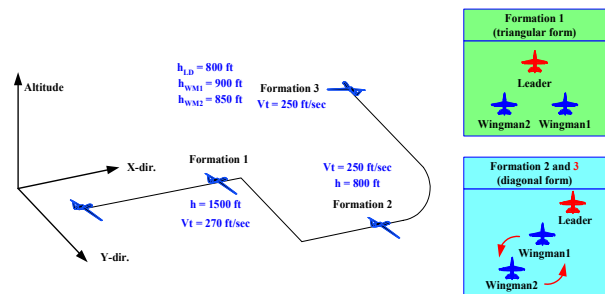


Fig. 5 Simulation scenario of formation flight.

4.3 Simulation results

In nonlinear simulation, each wingman initially flies in steady state at different position in three-dimensional space and the same velocity with leader. During formation flight, leader maneuvers following the predetermined trajectory shown in Fig. 5. At the end of three formation phases, each wingman has to maintain the assigned formation position with the same velocity and flight direction of the leader's one. The collision avoidance scheme is not considered in this simulation.

Initial value for nonlinear simulation of three aircrafts is referred in Table 1.

Simulation results according to formation flight scenario are depicted in Figs. 6-12. Fig. 6 shows the three-dimensional trajectories of leader and wingmen. The denoted three values of time in Fig. 6 are the final time of each formation phase. From the result showed in Fig. 7, two wingmen abruptly increase the velocity to form the desired formation reducing the position error caused by initial position. We can verify that the maintenance performance of altitude and flight direction of two wingmen is very accurate from the results of Fig. 8 and Fig. 9. Figs. 10-12 illustrate relative position time histories of two wingmen. The formation is completely formed within 50sec in spite of changing the formation form and various maneuvering of the leader aircraft.

Table 1 Initial condition for nonlinear simulation.

| | Leader | Wingman 1 | Wingman 2 |
|-------------------|------------|------------|------------|
| Velocity | 270 ft/sec | 270 ft/sec | 270 ft/sec |
| X-dir. position | 0 ft | -700 ft | -1000 ft |
| Y-dir. position | 0 ft | -300 ft | 500 ft |
| Altitude | 1500 ft | 1400 ft | 1600 ft |
| Flight path angle | 0 deg. | 0 deg. | 0 deg. |
| Heading angle | 0 deg. | 3 deg. | 0 deg. |

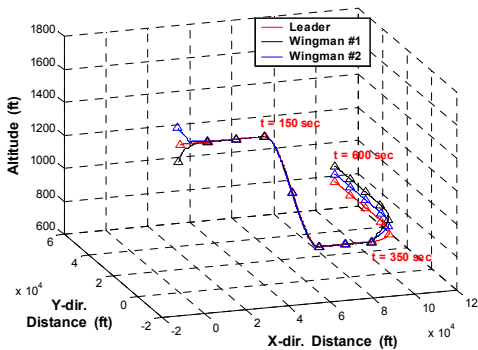


Fig. 6 Three dimensional trajectories during formation flight.

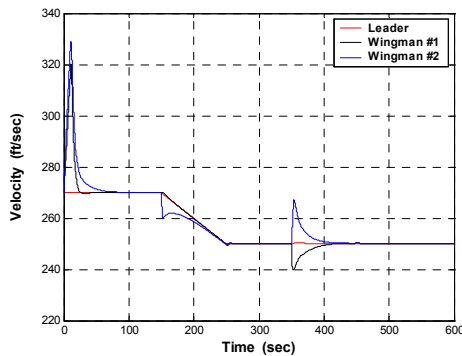


Fig. 7 Velocity time histories during formation flight.

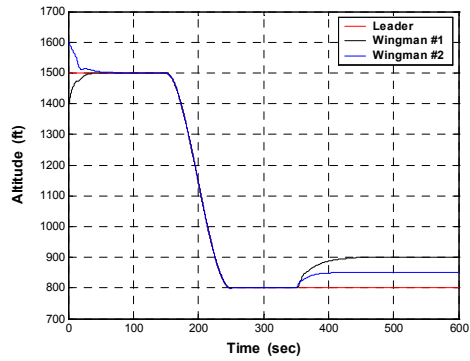


Fig. 8 Altitude time histories during formation flight.

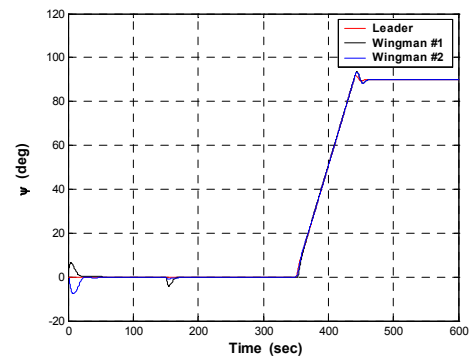


Fig. 9 Heading angle time histories during formation flight.

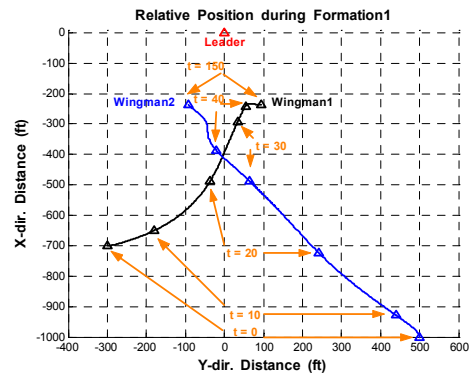


Fig. 10 Relative position variation in *Formation 1* phase.

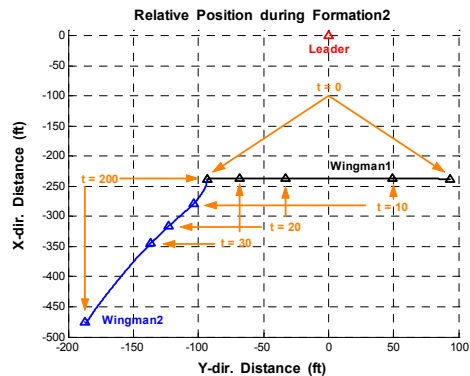


Fig. 11 Relative position variation in *Formation 2* phase.

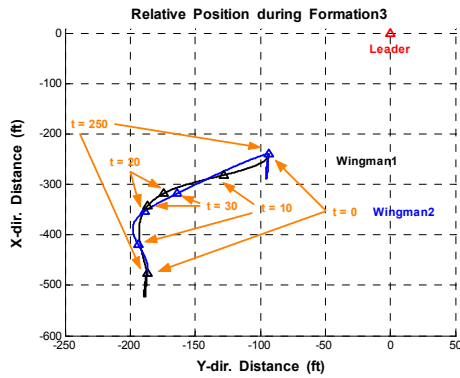


Fig. 12 Relative position variation in **Formation 3** phase.

5. CONCLUSION

In this paper, the three-dimensional guidance law for formation flight has been proposed. The new guidance law was derived using the concept of miss distance and Lyapunov stability theorem. The commands generated by the proposed guidance scheme are given in terms of velocity, flight path and heading angles. Thus, this scheme may be easily applied to the existing aircraft control system. Results from the nonlinear simulation of formation flight scenario with various formation forms, the new guidance law showed successful performance. The aircraft model used for formation flight simulation has full 6-DOF equation of motion and nonlinear aerodynamic and engine characteristics. The proposed guidance law will be useful to construct autonomous formation flight guidance law of multiple UAV.

The implementation of collision avoidance scheme and the performance degradation caused by communication delay are remained for further work.

ACKNOWLEDGMENTS

This paper was performed for Smart UAV Development Program, one of the 21st Century Frontier R&D Programs funded by the Ministry of Commerce, Industry and Energy of Korea.

REFERENCES

[1] F. Giulietti, M. Innocenti, M. Napolitano, and L. Pollini, "Dynamic and control issues of formation flight," *Aerospace Science and Technology*, Vol. 9, Issue 1, pp. 65-71, 2005.

[2] M. Pachter, J. J. D'Azzo, and A. W. Proud, "Tight formation flight control," *Journal of Guidance, Control, and Dynamics*, Vol. 24, No. 2, pp. 246-254, 2001.

[3] R. Sattigeri, A. J. Calise, and J. H. Evers, "An adaptive approach to vision-based formation control," *AIAA Guidance, Navigation, and Control Conference and Exhibit*, Austin, USA, 2003.

[4] M. J. Tahk, C. S. Park, and C. K. Ryoo, "Line of sight guidance laws for formation flight," *Journal of Guidance, Control, and Dynamics*, Accepted for publication as of June, 2004.

[5] F. Giulietti, L. Pollini, and M. Innocenti, "Autonomous formation flight," *IEEE Control Systems Magazine*, pp. 34-44, 2000.

[6] E. Yang, Y. Masuko, and T. Mita, "Dual-controller approach to three-dimensional autonomous formation control," *Journal of Guidance, Control, and Dynamics*,

Vol. 27, No. 3, pp. 336-346, 2004.

[7] B. L. Stevens and F. L. Lewis, *Aircraft Control and Simulation*, John Wiley & Sons, Inc., 1992.

[8] T. S. No, B. M. Min, R. H. Stone, and K. C. Wong, "Control and simulation of arbitrary flight trajectory-tracking," *Control Engineering Practice*, Vol. 13, Issue 5, pp. 601-612, 2005.

[9] P. Zarchan, *Tactical and Strategic Missile Guidance*, AIAA, Washington, DC, USA, 1992.

[10] J. J. Slotine and L. Weiping, *Applied Nonlinear Control*, Prentice-Hall International, Inc., 1991.

[11] T. S. No, J. E. Cochran, and E. G. Kim, "Bank-to-turn guidance law using lyapunov function and nonzero effort miss," *Journal of Guidance, Control, and Dynamics*, Vol. 24, No. 2, pp. 255-260, 2001.

[12] T. S. No, K. T. Chong, and D. W. Rho, "A lyapunov function approach to longitudinal control of vehicles in a platoon," *IEEE Transaction on Vehicular Technology*, Vol. 50, No. 1, pp. 116-124, 2001.